Optimization of the milling process for aluminum honeycomb structures

Tarik Zarrouk, Mohammed Nouari, Jamal-Eddine Salhi, Hamid Makich, Merzouki Salhi, Samir Atlati, Najim Salhi

Optimization of the milling process for aluminum honeycomb structures

[1]Tarik Zarrouk, Mohammed Nouari[2], Jamal-Eddine Salhi[1], Hamid Makich[2], Merzouki Salhi[i], Samir Atlati[3], Najim Salhi[1]
[1]Laboratory of Mechanics and Energy, Faculty of Sciences, First Mohammed University, Oujda/60000, Morocco
[2]Université de Lorraine, CNRS, LEM3, IMT, GIP InSIC, F-88100 Saint Dié des Vosges, France.
[3]ESTO, First Mohammed University, BP 473, Oujda, Morocco
*Corresponding author: *E-mail address:* zarrouk.tarik@ump.ac.ma

Abstract

The milling of aluminum honeycomb structures represents today an important scientific and technical research topic for many industrial applications: aerospace, aeronautic, automotive, and naval. The difficulties encountered when milling this type of materials are linked to the small thickness of the walls constituting the honeycomb cells and the ductility of the material structure. The milling of cellular composite structures requires specific and rigorous tools. In the present work, a 3D numerical modeling of the milling process of aluminum honeycombs has been developed using Abaqus / Explicit software. The effect of milling parameters, such as the spindle speed, the tilt angle, and the depth of cut have been particularly investigated in terms of cutting forces, surface integritu and chip morphology. To properly analyze and optimize the cutting process, experimental validation was done through milling tests with different cutting conditions. The comparison between numerical simulations and experimental tests shows that the three-dimensional model correctly reproduces the milling of this type of structure.

Keywords 3D Modeling. Honeycomb structure. Aluminium 5056. Milling process

1 Introduction

The use of aluminum honeycomb core for sandwich structures has increased significantly these last years in several industrial sectors such as aerospace, naval, and automotive [1,2]. One of the most widely used materials for honeycomb cores is the aluminium 5056. This growing interest for these honeycomb materials is mainly due to their low density and better mass/stiffness/strength ratio than metal alloys or conventional composite materials, [3,4]. Nevertheless, their machining remains poorly controlled due to the complexity of the phenomena involved in the cutting zone [5]. During the removal of the material and due to the heterogeneity and the anisotropy of these materials, the cutting process can generate damages that will increase with the repetition of the solicitations imposed on the structure in service and eventually lead to its degradation. These damages are mainly wall deformation, delamination, and thermal degradation [6,7]. The machining operations of this material are various, in particular turning, drilling, and milling. During the machining of this type of structures, the premature wear of the cutting tools is mainly due to the transfer of material to the cutting face of the tool, which favors the formation of the added edge (modification of the edge's geometry bonding) [8]. The formation of the built-up edge directly affects the quality of the machined surface. This phenomenon of material transfer to the tool is also called 'phenomenon of bonding'. In general, to machine, a material in the best conditions, the classical experimental method is often used based on the tool-material pair. The systematic use of this approach is costly in terms of investment (experimental device to be set up), time of occupation of the machine. However, once implemented, this approach provides results (cutting forces and cutter morphology, surface finish) rapidly. That also makes the experimental approach very expensive. For the understanding of the thermomechanical phenomena of cutting, this approach is not sufficient. Indeed, it does not give information on the local distribution (in the cutting zone) of the thermomechanical fields during cutting, data necessary for a more thorough study of the cutting process. Modeling and numerical simulation can be a fast, economical, and efficient way to reproduce the cutting process and to estimate the thermomechanical quantities characterizing the milling parameters of aluminum honeycomb structures. Several authors attributed the isotropic mechanical behavior to the shell element of aluminum honeycomb walls [9-12]. The mechanical and thermal characteristics of aluminum alloys require to use the well known Johnson-Cook viscoplastic behavior available in the literature [13,14]. Several authors have found a relation ship between the milling conditions, the morphology of the chips formed, the cutting forces and the quality

of the machined surface, this for different materials. Aydin et al. [15,16], studied the importance of ALE techniques to estimate more precisely cutting forces and chip morphology. They noticed that there is an important relation ship between mesh density, milling forces and chip segmentation. For aluminum honeycombs, the damage to the structure during machining is different. The ductile behavior of the aluminum walls and the thin walls favor the appearance of burrs in the cells. According to the standards, a burr is defined as a rough residue of material left outside the ideal geometric shape of an outer edge either by machining or by the forming process [17]. This constitutes "Degradation of the material" according to the standard reference NF E81-010 [18]. Several numerical and experimental works have studied the influence of cutting conditions on the morphology of the cutting edges, the surface quality, and the cutting forces [19,20]. The main objective of this work is to model and simulate the process of chip formation during milling of 5056 aluminum honeycomb structures, focusing on the influence of cutting conditions on cutting forces and chip morphology. In the first step, a validation of the FE model is established through experimental tests. Then a parametric analysis was performed to highlight the influence of the cutting conditions on the machinability of this type of structure.

2 Implementation of the numerical simulation

The aluminum honeycomb with a density of 49 kg/m^3 has been chosen because it is the most often used configuration for aeronautical panels and an important industrial grade aluminium honeycomb due to its high mechanical performance. The geometric configuration of the 5056 aluminum honeycomb is characterised of by a thickness of 11 mm, a width of 25 mm, a length of 32 mm, and a cutting depth of 6mm (see Fig.1). Table 1 shows the geometric characteristics of the aluminum honeycomb core.

Table 1 Geometrical characteristics of honeycomb core

Density [Kg/m^3]	Cell size l [mm]	Wall size t [mm]	Angle θ [°]
49	3.2	0.06	120

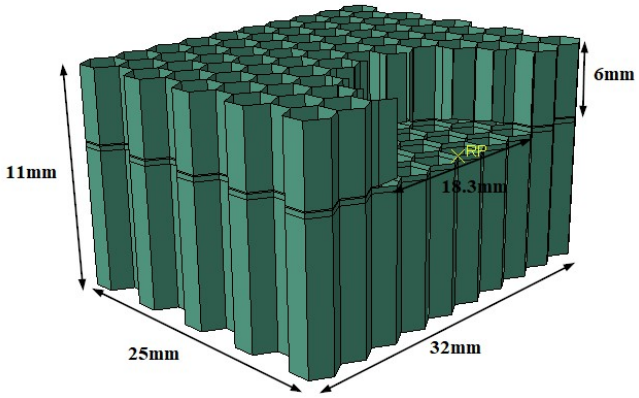

Fig 1. Geometric characteristics of the Aluminum honeycomb core.

The cutting tool for milling aluminum honeycomb is a combined tool consisting of two parts. The upper part has a diameter of 16 mm with 10 helices containing chip breakers and a lower part consisting of a conical tungsten carbide disc containing 55 teeth. The geometrical dimensions are shown in Fig. 2(a).

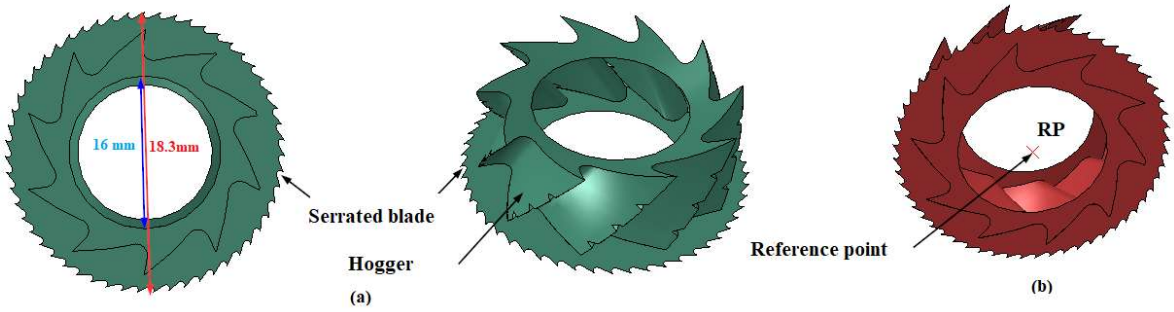

Fig 2. (a)- The CZ10 cutting tool used for milling the Aluminum honeycomb core. (b)- Milling conditions applied to the RP reference point of the cutting tool: N is the rotation speed and f is the feed rate.

3 Modelling of the cutting process

3.1 Modelling set up

Within the framework of milling of the structures in aluminum honeycomb 5056, a 3D modeling is set up using the FE numerical code Abaqus/Explicit in its version 6.17. The Lagrangian formulation takes into account the interaction between the cutting tool and the honeycomb structure. The tool is modeled as a rigid material, which means the non-attribution of mechanical and thermal properties to it. The feed rate f and the rotational speed N were applied at the level of the reference point where the cutting forces are calculated. Regarding the behavior of the cutting tool, it was considered as a rigid body in all simulations, (See Fig. 2(b)). A tool location is provided in the honeycomb structure, respecting its geometry with a cutting depth of 6 mm. To reduce CPU calculation time. At the start of the simulation, we assigned a contact between the cutting tool and the structure to be machined, while respecting the specific geometry of the cutter and the serrated blade. The boundary conditions are chosen according to the experimental protocol performed. To avoid the sliding, the structure is embeded. Moreover, the movement of the workpiece is canceled along the two directions *X* and *Y* (Fig. 3).

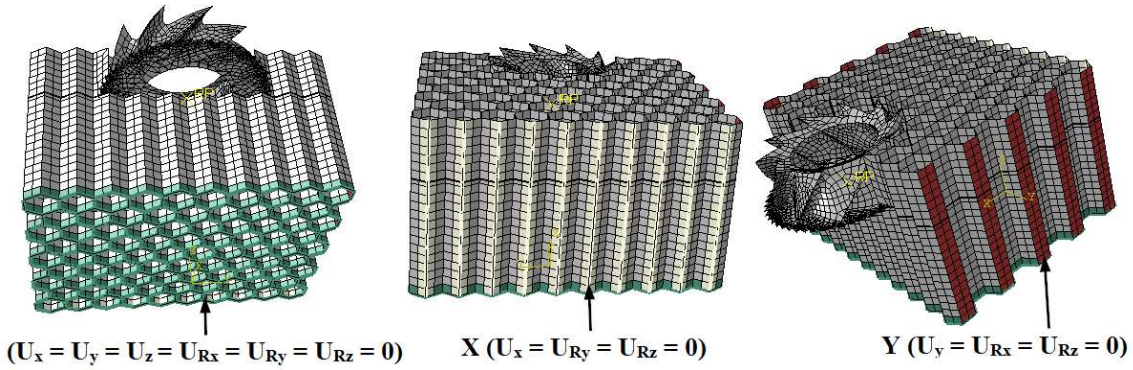

Fig 3. Boundary conditions used for the finite element model.

The aluminum honeycomb core is meshed using conventional 4-node shell elements with reduced integration of type S4R, while the cutting tool is meshed by rigid quadrangular elements of type R3D4 (Fig. 4).

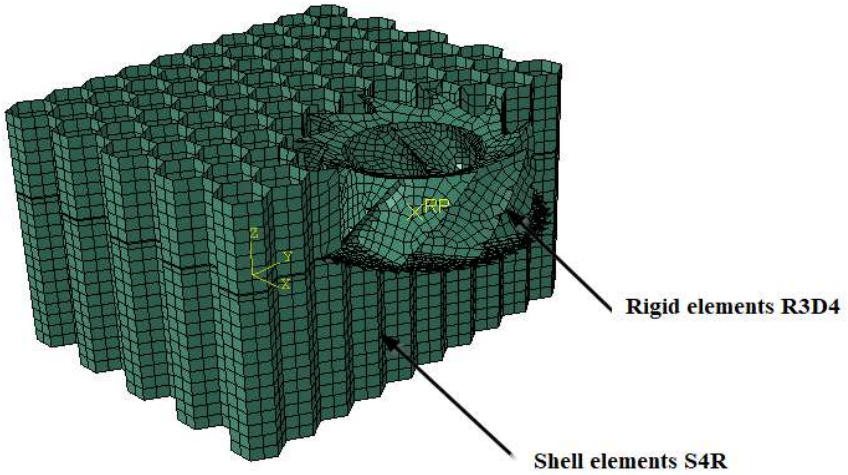

Fig 4. Mesh used in the EF model. The directions of the cutting forces Fx, Fy and Fz are defined according to the direction of axes X, Y and Z.

3.2 Johnson-Cook type behavior model

The aluminum honeycomb is made of 5056 aluminum sheets, and they are represented as shell elements during the simulation. The aluminum 5056 sheets are homogeneous with a mechanical behavior similar to that of bulk

aluminum. Generally, aluminum is modeled by a thermo-visco-plastic law given by JohnsonCook Eq. (1). This model is decomposed into three parts representing the effect of strain hardening, the effect of the strain rate (effect of viscosity), and thermal softening. It is represented by the following law [13,21,22]:

$$\bar{\sigma} = [A + B\bar{\varepsilon}^{n}][1 + Cln(\frac{\dot{\bar{\varepsilon}}}{\dot{\bar{\varepsilon}}_0})]\ [1- (\frac{T-T_0}{T_f-T_0})^{n}] \quad (1)$$

with A, B, n, C, and m as constants of the machined material to be determined experimentally. $\dot{\bar{\varepsilon}_0}$ is the reference strain rate. T_f and T_0 are the melting and reference temperatures, respectively.

Table 2 summarizes the various mechanical properties of 5056 aluminum attributed to the honeycomb walls [13].

Parameters Properties	Value
Reference density (g/cm3)	2.78000E+00
Bulk modulus (kPa)	7.90600E+07
Reference temperature (K)	3.00000E+02
Specific heat (J/kg K)	8.75000E+02
Shear modulus (kPa)	2.76000E+07
Yield stress (kPa)	1.40000E+05
Hardening constant (kPa)	4.26000E+05
Hardening exponent	3.40000E−01
Strain rate constant	1.50000E−02
Thermal softening exponent	1.00000E+00
Melting temperature (K)	6.83000E+02
Ref. strain rate (/s)	1.00000E+00
Strain rate correction	1st Order
Plastic strain	0.03500E+00

The J-C thermo-viscoplastic model given by Eq. (1) is used to reproduce the workpiece's behavior. To take into account the drop in stress after a certain value of plastic deformation, the JC damage law (JCD) given by Eq. (2), is defined. The use of this damage law is intended to allow the simulation of the chip formation as well as its scalloping and fragmentation. A failure is initiated in the material once the parameter DJC is equal to 1 (initiation of damage).

$$\varepsilon_f = [d_1 + d_2\varepsilon^{[-d_3\frac{p}{\bar{\sigma}}]}]\ [1+d_4 ln(\frac{\dot{\bar{\varepsilon}}}{\dot{\bar{\varepsilon}}_0})]\ [1- d_5(\frac{T-T_0}{T_f-T_0})] \quad (2)$$

with d_1, d_2, d_3, d_4, and d_5, the damage parameters of the Johnson-Cook model associated with the machined material.

3.3 Tool–Workmaterial interface behaviour (interface friction law)

The behavior at the tool/chip interface is the one that governs the chip formation process. It represents the scientific lock for the modeling of metal cutting. The tool/chip contact is not yet mastered from point of view of modeling. Because it is influenced by several factors, including temperature, contact pressure, local sliding speed, and the behavior of the workpiece and the cutting tool materials. To properly estimate cutting forces and chip morphology, it is essential to understand the friction process between the cutting tool and the workpiece Various friction laws have been proposed in order to simulate the behavior of matter at the interface chip tool. It has been shown in studies [23] that the Coulomb law is among the most suitable models to describe tool-chip contact in machining. In this work, the friction at the tool-part interface is modeled by Coulomb's law (see Eq. (3)). The following relation ship relates the normal σ_n and tangential τ_f frictional stresses:

$$\tau_f = \begin{cases} \mu\,\sigma_n & \text{if } \mu\,\sigma_n \prec \tau_{max} \\ \tau_{max} & \text{if } \mu\,\sigma_n \geq \tau_{max} \end{cases} \quad (3)$$

Where μ is the friction coefficient and τ_{max} is the limit shear stress.

We note that the coefficient of friction adequate to correctly reproduce the experimental trends is $\mu = 0.22$.

The greatest source of variation in energy consumed during machining is the cutting force. This makes it a reasonable choice as a criterion for cutting performance. Therefore, knowing the characteristics and variables that

influence the cutting force is essential. As part of our work, depending on our objectives, we need to know the overall cutting force which can be calculated by the following formula [24]:

$$FAvg = \sqrt{F_x^2 + F_y^2 + F_z^2} \quad (4)$$

4 Results and discussion

4.1 Mesh size study

The choice of the mesh size is essential in numerical simulation. This is mainly due to its direct influence on the reliability of the obtained results and the CPU computation time. In the case of the refined mesh, the FE formulation with full integration generates a longer calculation time but gives robust results. On the contrary, in the case of the coarse mesh, the computation time is reduced but the calculation gives not accurate results. That is why, in each study it is necessary to find the best compromise between the chosen mesh size, the computing CPU time, and the accuracy of the calculated results. In this section, the effect of the mesh size on the cutting forces during the simulation of the milling of aluminum honeycomb structures is investigated. The cutting conditions used are presented below. Eight numerical simulations with a mesh size between 0.2-0.9 mm were performed. The cutting forces in the eight cases are plotted in Figs. 5 and 6 and compared to each other.

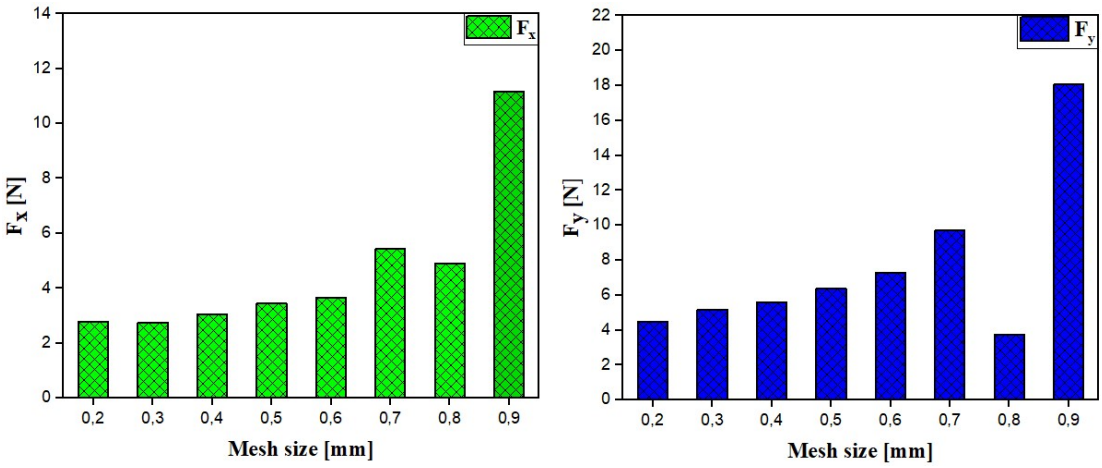

Fig 5. Evolutions of the cutting force components, F_x and F_y for f = 3000 mm /min, N= 23000 rpm, depth of cut a_p= 6mm. The directions of the cutting forces Fx, Fy and Fz are defined according to the direction of axes X, Y and Z as shown in Figure 4.

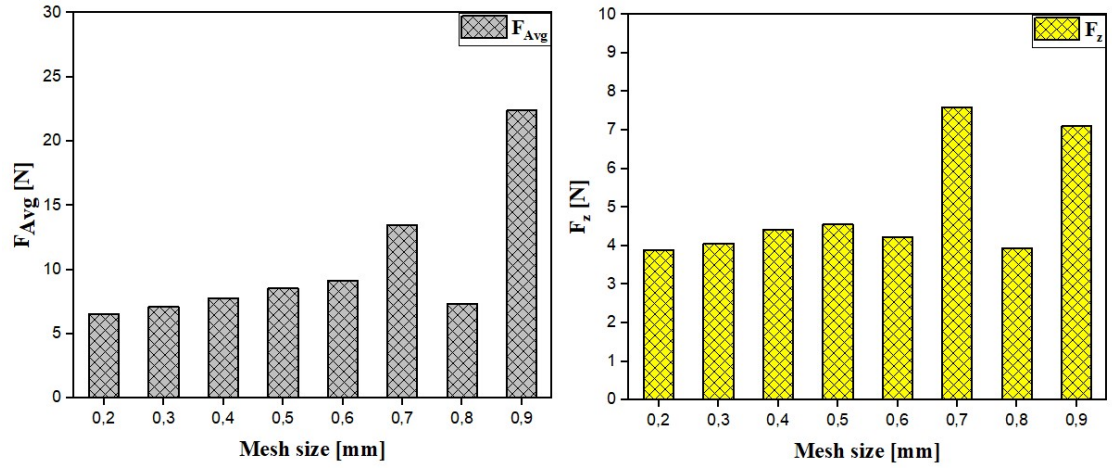

Fig 6. Evolutions of the cutting force components, F_z and F_{Avg} for f = 3000 mm /min, N= 23000 rpm, depth of cut a_p= 6mm. The directions of the cutting forces Fx, Fy and Fz are defined according to the direction of axes X, Y and Z as shown in Figure 4.

It has been found that the components of the cutting force F_x, F_y and F_z are not stable between the mesh size 0.7 and 0.9 mm, so that the forces decrease between 0.7 and 0.8 mm and then increase between 0.7 and 0.9 mm. This disagreement is explained by the strong dependence on the force of the elastic return of the walls at the level of the flank face. Thus, when the element reaches the breaking point, it is removed. This removal is accompanied by a loss of contact between the material and the cutting tool, which reduces the cutting forces. Indeed, the elastic return of the uncut walls causes resistance in the opposite direction of rotation of the tool and therefore in reality generates an increase in the cutting force. The obtained results shows a stabilization of the cutting forces and their components when the mesh size varies between 0.2 and 0.6 mm. In addition, small mesh elements notably have a lower ability to "resist" deformation. Therefore, mesh distortion problems are likely to occur more quickly, thus causing calculations to stop. Therefore, we have adopted a mesh size compatible with reasonable accuracy and efficiency. The mesh size that has been chosen in the Abaqus library (about 0.5mm) must be reconsidered (0.2 mm) to meet the best compromise.

4.2 Effect of the rotation speed on the cutting forces

It is well known that cutting speeds generate fluctuations in cutting force, chips morphology, and generated surface quality [25,26]. To highlight the effect of the rotation speed on cutting forces, a comparison between the numerical and experimental cutting forces is carried out [27]. The numerical simulations were performed with four rotation speeds (2000, 10000, 15000, and 23000 rpm) and a feed rate of 3000 mm/min. A location the tool is also provided in the honeycomb structure respecting its geometry with a cutting depth of 6 mm. The tool chosen for this simulation is the combined tool given its behavior characterized during the experimental phase (see Fig. 2). For each simulation, the first phase of penetration of the tool in the material is neglected. The numerical simulations were carried out during 0.04 s, which represents a milling path of 2 mm. The obtained results are shown in Fig. 7 and Fig. 8.

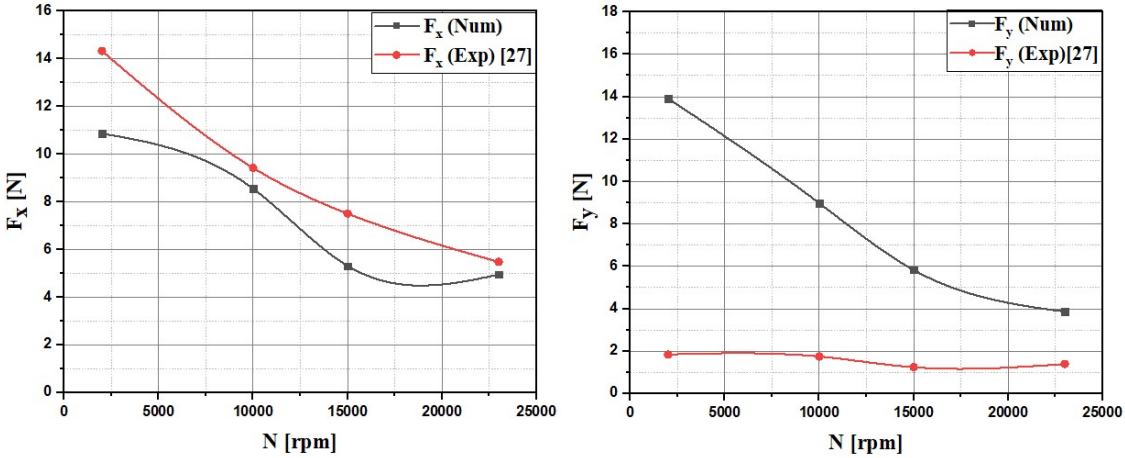

Fig 7. Evolutions of components F_x and F_y.

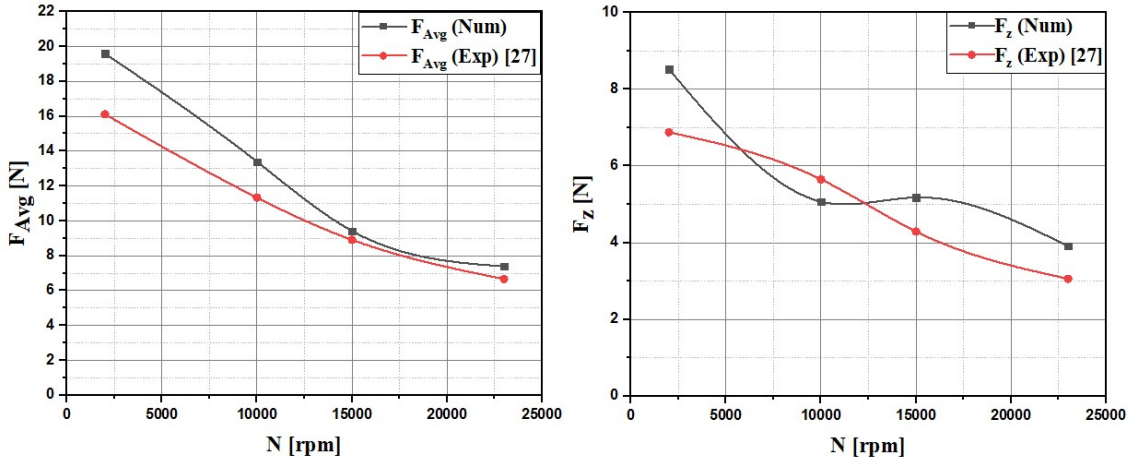

Fig 8. Evolutions of components F_x and F_y.

The obtained results by the numerical simulations generally follow the experimental course of the cutting force components, the latter decrease with the increase of the rotation speed (spindle speed N). The cutting forces are important for low rotation speeds. This is due to the accumulation of walls in front of the upper part of the cutting tool. This accumulation occurs because of the elastoplastic properties of the aluminum. The elastoplastic behavior ensured by Johnson-Cook's law means that this accumulation persists because of the plastic deformation of the walls before reaching failure. The small contact between the tooth of the tool and the honeycomb wall as well as the alveolar geometry which allows better heat dissipation. Thus the importance of thermal softening on the behavior of the material. The results obtained by the numerical simulation generally follow the experimental shape of the components F_x and F_z of the cutting force. On the contrary,The F_y component is not compatible with the experimental results due to removing the damaged elements and the loss of contact with the cutting tool. By comparing the components of the cutting force predicted during milling of the Nomex structure (composite material) and this under the same cutting conditions indicated above, the component F_z is not important but rather the components F_x and F_y [28]. This can be explained by the effect of the geometry of the tool, which has teeth at the level of the cutting edge, and the behavior of the Nomex structure, which is characterized by out-of-plane resistance. Finally, numerical modeling represents a good prediction overall in terms of cutting forces.

4.3 Effect of cutting depth on cutting forces and cutter morphology

The most influential parameters on machining are the cutting forces and depth of cut, regardless of the material being machined [29,30]. In this sense, it has been shown that the machining forces increase with increasing the depth of cut a_p. In this paragraph, a numerical study has been carried out to verify the effect of the depth of cut a_p on the cutting forces and the size of the chip when milling aluminum honeycomb structures. Indeed, a series of simulations were made under the same milling conditions mentioned below. The numerical simulations were performed during 0.04 s, which represents a milling path of 2 mm. Only the cutting depth a_p was varied. The depths of cut examined are 2, 6, 12 mm. The calculated results are shown in Fig. 9.

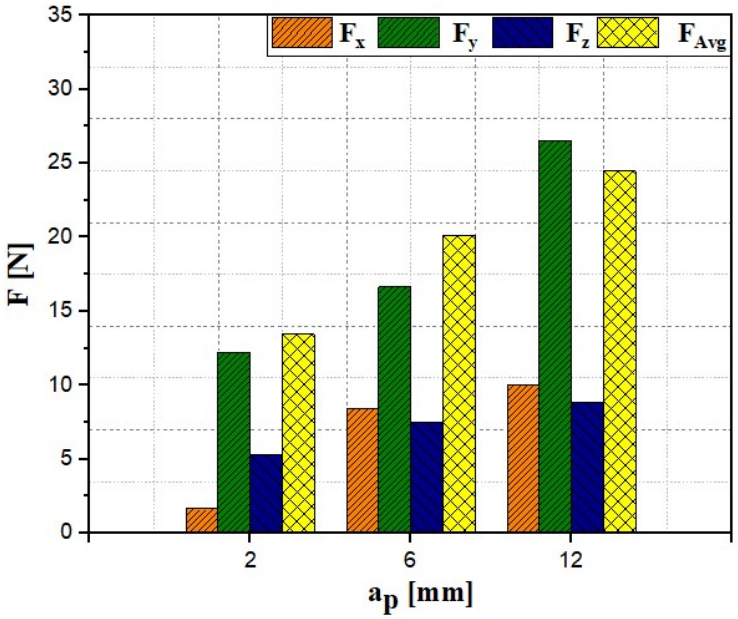

Fig 9. Evolutions of the cutting force components, F_x, F_y, F_z and F_{Avg} for f = 3000 mm /min, N=2000 rpm.

Nevertheless, it can be noted that the cutting force strongly increases with the depth of cut for all the simulations involved. The cutting forces vary significantly when the cutting depth increases from 2 to 12mm so that the cutting force and its components are approximately tripled. This is consistent with the findings in the literature of Wang et al. et Jenarthanan et al. [24,31]. Regarding the chip size, the three-dimensional numerical model allowed us to visualize the chip morphology for each of the tested conditions resulting from the milling of the aluminum honeycomb structures. Figs. 10, 11, and 12 show the evolution of the chip size as a function of the cutting depth a_p. It can be seen that the cutting depth strongly impacts the chip size. Indeed, the latter increases with the increase of the depth of cut. These trends can obviously be explained by the fact that at a greater depth of cut, a greater volume of material is machined, hence an increase in the cutting force can be immediately observed, [32,33].

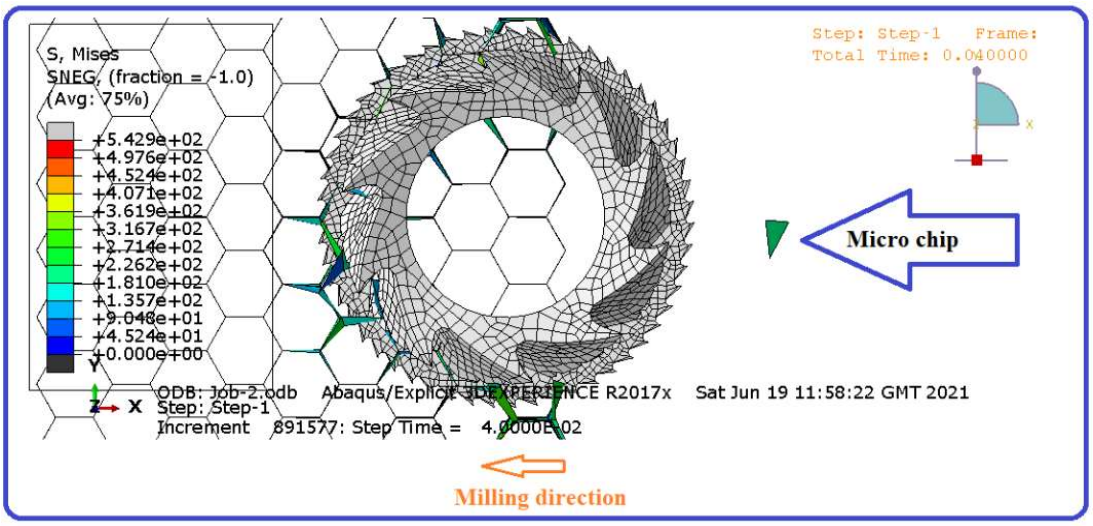

219

220 **Fig 10.** Effect of the cutting depth on the morphology of obtained chips: f = 3000mm / min, 2000 rpm, a_p = 2mm.

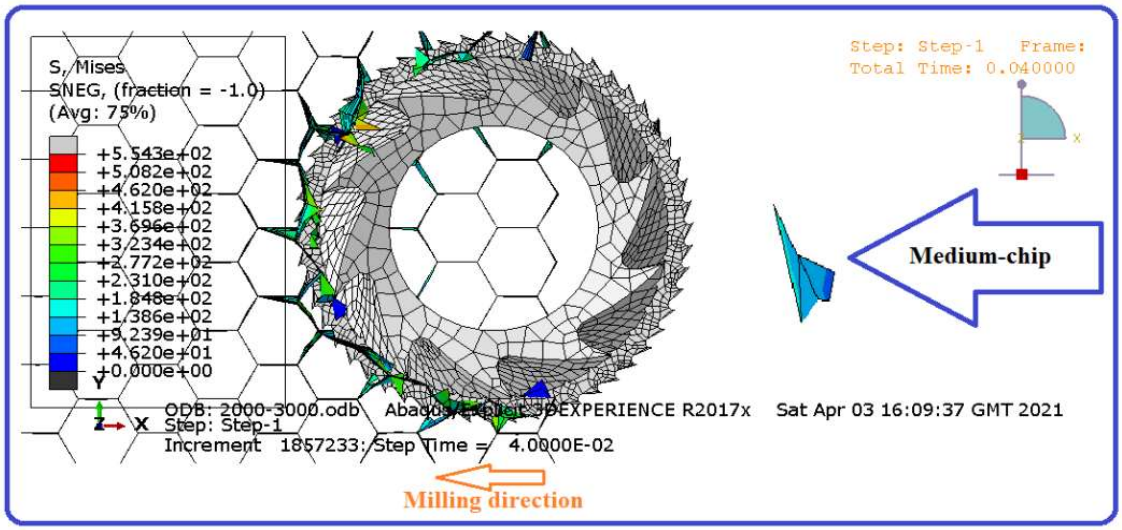

221

222 **Fig 11.** Effect of the cutting depth on the morphology of chips: f = 3000mm / min, N= 2000 rpm, a_p = 6mm.

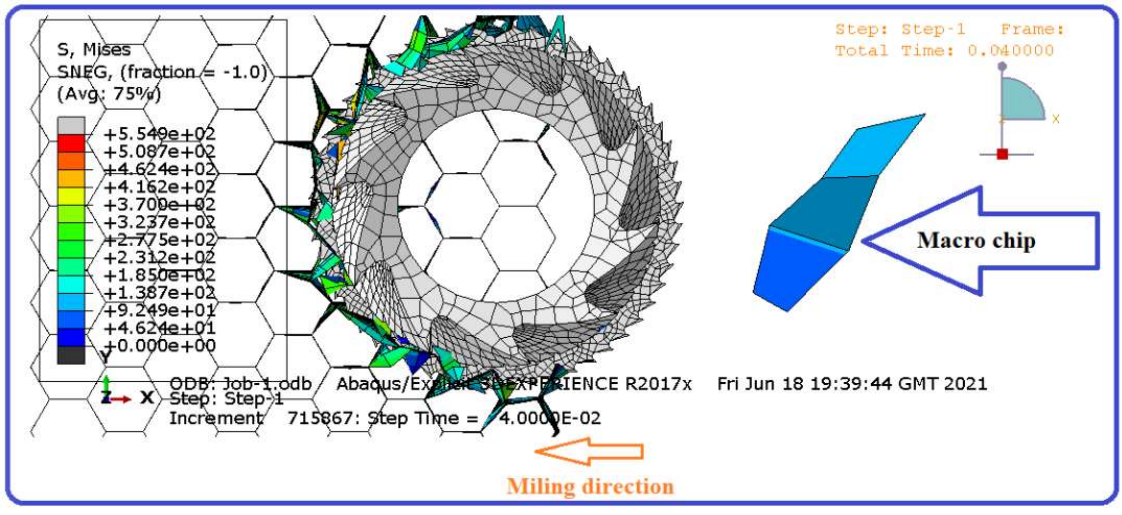

223

224 **Fig 12.** Effect of the cutting depth on the morphology of chips: f = 3000mm / min, N= 2000 rpm, a_p = 12 mm.

225 ***4.4 Influence of the tool tilt angle on the cutting forces***

We propose to determine the most favorable tilt of the cutting tool concerning the surface of the part. In order to minimize vibration and maximum force values, seek surface quality performance and limit cutting tool wear, a numerical study was conducted to verify the effect of the tilt angle on the cutting forces. Four tilt angles were studied 0°, 5°, 10°, and 15°. The used cutting conditions are presented below. The milling time is about 0.04 s, which represents a milling distance of 2mm. The obtained results are shown in Figs. 13 and 14.

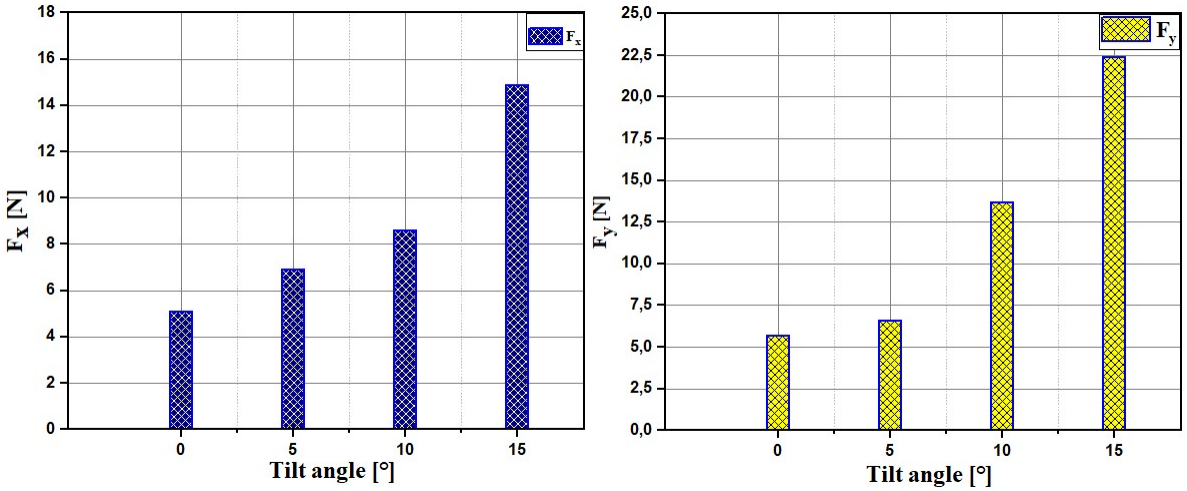

Fig 13. Evolutions of components, F_x and F_y for f = 3000 mm /min, N=15000 rpm, depth of cut a_p= 6 mm.

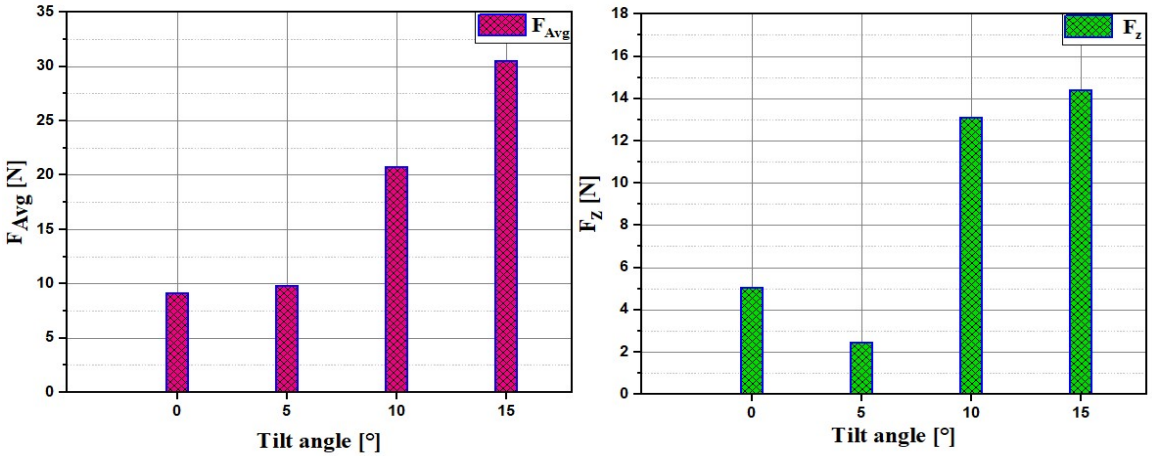

Fig 14. Evolutions of components, F_x and F_y for f = 3000 mm /min, N=15000rpm, depth of cut a_p= 6 mm.

According to the obtained results, we found a slight variation of the cutting forces with the increase in the tilt angle taken between 0° and 5°. This trend is also found for all the simulations performed. However, the cutting force and its components are approximately tripled when the cutting angle increases from 5° to 15°. Also, it should be noted that the F_z component is not important but rather the F_y and F_z components. This is explained by the tool geometry and the elastoplastic behavior of aluminum 5056. Finally, the high angle cutting tool generates higher cutting forces than those found with the 0° cutting angle, so the wear of the cutting tool is premature for high tilt angles. In this regard, close correlations in the form of third order polynomials are formulated and developed from the results of Figs 13 and 14. It is important to emphasize that these correlations are only applicable to the machining conditions indicated above.

$$F_x = 0{,}0063\ \alpha^3 - 0{,}0972\ \alpha^2 + 0{,}6903\ \alpha + 5{,}1 \quad \text{and} \quad R^2 = 1 \tag{5}$$

$$F_y = -0{,}0061\ \alpha^3 + 0{,}2168\ \alpha^2 - 0{,}7563\ \alpha + 5{,}7 \quad \text{and} \quad R^2 = 1 \tag{6}$$

$$F_z = -0{,}0302\ \alpha^3 + 0{,}7188\ \alpha^2 - 3{,}3607\ \alpha + 5{,}05 \quad \text{and} \quad R^2 = 1 \tag{7}$$

$$F_{Avg} = -0{,}0154\ \alpha^3 + 0{,}4358\ \alpha^2 - 1{,}659\ \alpha + 9{,}16 \quad \text{and} \quad R^2 = 1 \tag{8}$$

R^2 represent the coefficient of determination, α represents the tilt angle.

4.5 Effect of rotation speed on the chip morphology

During a milling operation, the chip formation mechanism involves strong interactions between the cutting tool and the structure to be machined. The material behavior law directly impacts the formation of chips, the geometry of the cutting tool, and the used cutting conditions [25]. In practice, the chip formation process is still very difficult to visualize. However, numerical modeling by 3D finite elements facilitates the visualization of the different stages of the chip formation process. In this paragraph, a numerical study was performed to investigate the influence of rotation speed on the morphology of the generated chips. Two rotation speeds were examined, N = 2000 rpm and 23000 rpm, with a feed rate of 3000 mm/min. The milling operation time is 0.04 s which represents a 2 mm gap. Figs. 15 and 16 show the accumulation of the material in front of the cutting tool according to the milling conditions proposed above.

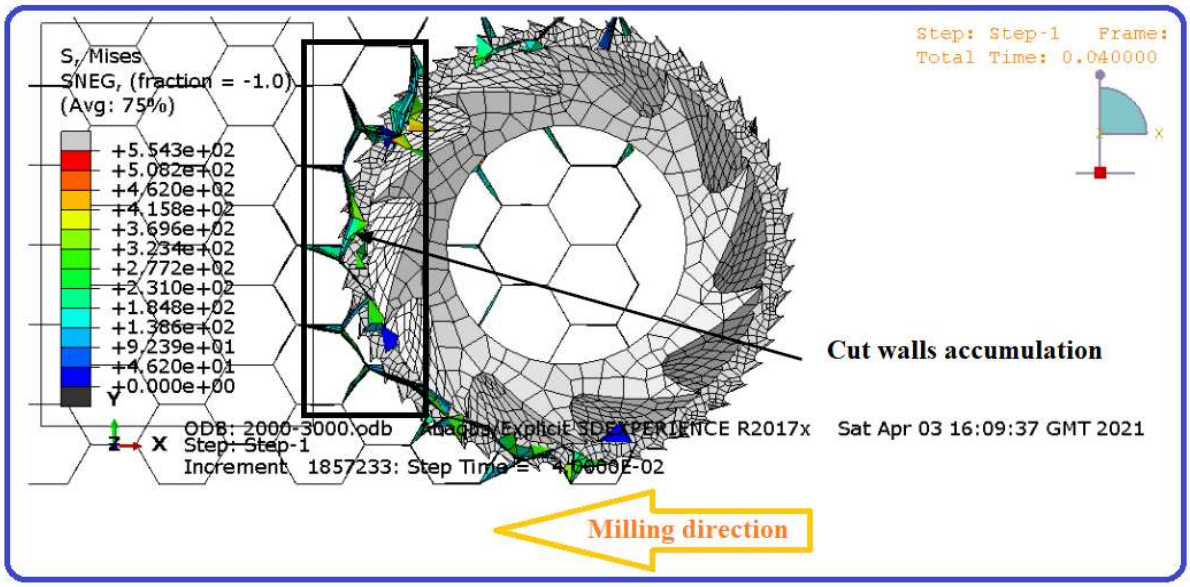

Fig 15. Accumulation of material in front of the cutting tool, cutting conditions: f = 3000 mm / min, N = 2000 rpm.

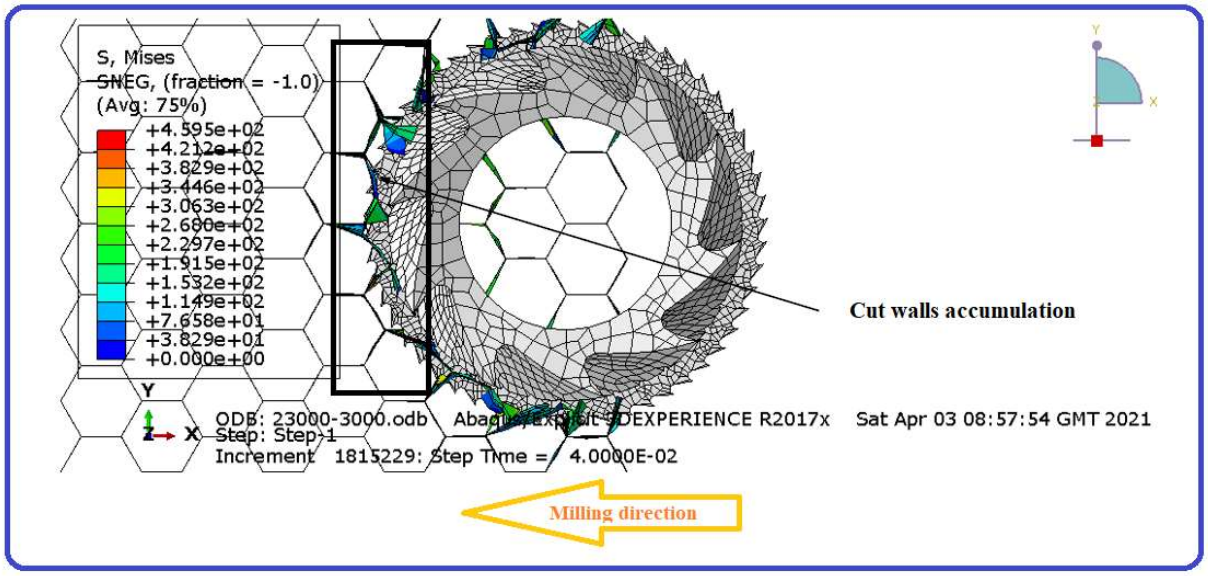

Fig 16. Accumulation of material in front of the cutting tool, cutting conditions: f = 3000 mm/min, N = 23000 rpm.

The difference in diameters between the two components of the cutting tool (Hogger + serrated blade) means that the cutting of the honeycomb structure is done in several stages. The first element (serrated blade) that is in contact with the walls of the honeycomb. The latter begins by cutting the walls by turning and advancing the material. Thus, the cutting and separation of the wall elements is done by damage and friction. The advancement and rotation of the tool causes the stresses to increase in the walls elements. At each increment, the failure criteria are checked

if they are met, damaged elements are removed to form the chip. In the next step, the detached walls of the structure float on the upper face of the serrated blade until they reach the shredder (Hogger). Thus, the shredder, through these 10 propellers, cuts these walls into several pieces. The role of this shredder is to shred the walls and thus free the passage of the tool to advance through the material. As with composite materials (eg Nomex), this accumulation of material has an influence on the cutting forces and on the shape of the chips generated [25]. The figs. 15 and 16 show the build-up of material in front of the cutting tool for two cutting conditions. The condition f=3000 mm/min, N= 2000 rpm show the greatest accumulation of material in front of the shredder, which will decreases by increasing the rotation speed to 23000 rpm. The elastoplastic behavior provided by the Johnson-Cook law makes this accumulation persist because of the plastic deformation of walls before reaching the rupture point. This elastoplastic behavior also generates the phenomenon of bending of the walls because of the ductility of aluminum and its capacity to deform plastically. This bending phenomenon is reproduced in the numerical simulations carried out for all the used cutting conditions. It is essentially caused by the ductile behavior of the aluminum walls and by the geometric characteristics of the honeycomb. Jaafar et al. made the same conclusion in their experimental studies [27].

5 Conclusion

Thanks to a 3D finite element model based on the Lagrangian approach, the effect of cutting conditions on cutting forces and chip morphology was fully analysed when milling aluminum honeycomb structures. The developed model takes into account the complex interactions between the alveolar cells and the geometry of the cutting tool. First of all, the appropriate mesh size has been chosen respecting the good compromise between the CPU calculation time and the reliability of the calculated results. Thus the size of the mesh retained in this work is about 0.2mm. The validation of the model was carried out by comparing the cutting force and its components resulting from the numerical simulation with the results obtained experimentally. The convergence was noticed between the cutting forces calculated numerically and the results obtained experimentally, so that the cutting forces decrease with high spindle speeds. Thus, the numerical model is more profitable and efficient. The proposed numerical model allows us to verify the influence of the depth of cut on the cutting forces and the morphology of the generated chip. From this work, the following conclusions can be drown :

- The cuting forces and the depth of cut has a direct influence on the chip size, so that these qantities increase with the depth of cut.
- The three-dimensional model allowed us to study the influence of the tool tilt on the components of the cutting forces. The cutting forces are important for large tilt angles. Thus, it has been shown that it is possible to avoid negative effects and improve the cutting force results by decreasing the tilt angle and avoiding the tool wear.
- The influence of the spendle speed on the accumulation of the material in front of the cutting tool was clearley established. The obtained results allow to conclude that the rotation speed influences the morphology of the chip so that the low rotation speeds generate a more important accumulation and vice versa.
- The results in terms of cutting forces, chip morphology, surface quality and their dependance on the cutting conditions make it possible to determine the range of validity of the cutting tool. This process, called the tool-material pair, allows a correct operating area of the tool to be defined.
- The study of the variation of the cutting forces as a function of machining conditions allows to give a relevant information on the surface quality and chip morphology
- From an industrial point of view, the optimisation of machining operations needs long and very expensive experiments to test different configurations. The proposed 3D modelling can then be a very useful and helpful tool to run numerical simulations for different test plans in a short time and with low cost.

Declarations

Funding

Not applicable

Competing interests

The authors declare that they have no competing interests

Availability of data and materials

Not applicable.

Code availability

Not applicable.

Ethical Approval

Not applicable

Consent to Participate

Not applicable

Consent to Publish

Not applicable

Authors' contributions

Not applicable.

References

[1] Cognard P (2003) Collage des composites. Ed. Techniques Ingénieur

[2] Reyne M (1998) Les composites dans les sports et les loisirs. Ed. Techniques Ingénieur

[3] Dessarthe A (1992) Assemblage des matériaux composites, structures sandwichs et matiéres plastiques

[4] Jansons J, Kulakov V, Aniskevich A, Lagzdiņš A Structural (2012) Composites− From Aerospace to Civil Engineering Applications. Innovations and Technologies News 4(17): 3-12

[5] Dessarthe A (1999) Usinage des composites à matrice polymère. Tech. l'Ingénieur

[6] Geng D, Zhang D, Xu Y, He F, Liu D, Duan Z (2015) Rotary ultrasonic elliptical machining for side milling of CFRP: Tool performance and surface integrity. Ultrasonics 59: 128-137

[7] Teti R (2002) Machining of Composite Materials. CIRP Annals 51(2): 611-634

[8] Zhao H, Elnasri I, Abdennadher S (2005) An experimental study on the behaviour under impact loading of metallic cellular materials. Int. J. Mech. Sci 47(4-5) 757-774

[9] Chandler H.E (1989) Machining of Metal-Matrix Composites and Honeycomb Structures. Asm handbook 16: 893-901

[10] Qiu K, Ming W, Shen L, An Q, Chen M (2017) Study on the cutting force in machining of aluminum honeycomb core material. Compos. Struct 164: 58-67

[11] Gao Y, Ko J.H, Lee H.P (2018) 3D coupled Eulerian-Lagrangian finite element analysis of end milling. The International Journal of Advanced Manufacturing Technology 98 (1): 849-857

[12] Daoud M, Chatelain J. F, Bouzid A (2015) Effect of rake angle on Johnson-Cook material constants and their impact on cutting process parameters of Al2024-T3 alloy machining simulation. The International Journal of Advanced Manufacturing Technology 81(9): 1987-1997

[13] Kang P, Youn S. K, Lim J. H (2013) Modification of the critical projectile diameter of honeycomb sandwich panel considering the channeling effect in hypervelocity impact. Aerospace Science and Technology 29(1): 413-425

[14] Huang W,Zhang W, Li D, Ye N, Xie W, Ren P (2016) Dynamic failure of honeycomb-core sandwich structures subjected to underwater impulsive loads. European Journal of Mechanics-A/Solids 60: 39-51

[15] Aydin M, Köklü U (2017) Identification and modeling of cutting forces in ball-end milling based on two different finite element models with Arbitrary Lagrangian Eulerian technique. The International Journal of Advanced Manufacturing Technology 92: 1465-1480

[16]Aydin M, Köklü U (2020) Analysis of flat-end milling forces considering chip formation process in high-speed cutting of Ti6Al4V titanium alloy. Simulation Modelling Practice and Theory 100: 102-039

[17] Régnier T, Fromentin G, Outeiro J, Marcon B, d'Acunto A, Crolet A (2016) Etude de la formation des bavures en coupe orthogonale à l'outil carbure dans un alliage d'Aluminium – Silicium

[18] Boussaha A (2007) Etude expérimentale des paramètres influants le serti des boites métalliques: Cas de l'unité BENPACK–Batna. Dissertation, Université de Batna 2

[19] Tiabi A (2010) Formation des bavures d'usinage et finition de pièces. Dissertation, École de technologie supérieure
[20] Niknam S. A (2013) Burrs understanding, modeling and optimization during slot milling of aluminium alloys Dissertation, École de technologie supérieure
[21] Crupi V, Epasto G, Guglielmino E, Mozafari H, Najafian S (2014) Computed tomography-based reconstruction and finite element modelling of honeycomb sandwiches under low-velocity impacts, J. Sandw. Struct. Mater 16 (4) :377-397
[22] Johnson G.R, Cook W.H (1985) Fracture characteristics of three metals subjected to various strains, strain rates, temperatures and pressures. Eng. Fract. Mech 21(1): 31-48
[23] Atlati S (2012) Développement d'une nouvelle approche hybride pour la modélisation des échanges thermiques à l'interface outil copeau : Application à l'usinage de l'alliage d'aluminium aéronautique AA 2024-T351. Dissertation, Université de Lorraine, France.
[24] Jenarthanan M.P, Jeyapaul R (2013) Optimisation of machining parameters on milling of GFRP composites by desirability function analysis using Taguchi method. Int. J. Eng. Sci and Technology 5(4): 22-36
[25] Zarrouk T, Salhi J.E, Atlati S, Nouari M, Salhi M, Salhi N (2021) Modeling and numerical simulation of the chip formation process when machining Nomex. Environmental Science and Pollution Research:1-8.
[26] Jaafar M, Atlati S, Makich H, Julliere B (2017) A 3D FE modeling of machining process of Nomex® honeycomb core: influence of the cell structure behaviour and specific tool geometry. *Procedia Cirp* 58 : 505-510.
[27] Jaafar M (2018) Étude expérimentale et simulation numérique de l'usinage des matériaux en nids d'abeilles : application au fraisage des structures Nomex® et Aluminium. Dissertation, Université de Lorraine, France.
[28] Zarrouk T, Salhi J.E, Atlati S, Nouari M, Salhi M, Salhi N (2021) Study on the behavior law when milling the material of the Nomex honeycomb core. Materials Today: Proceedings 45(8): 7477-7485
[29] Sahare S.B, Untawale S.P, Chaudhari S.S, Shrivastav R.L, Kamble P.D (2017) Experimental investigation of end milling operation on Al2024. Mater. Today Proc 4(2): 1357-1365
[30] Moshat S, Datta S, Bandyopadhyay A, Pal P (2010) Optimization of CNC end milling process parameters using PCA-based Taguchi method, Int. J. Eng. Sci. Technol 2(1): 95-102
[31] Wang D.H, Ramulu M, Arola D (1995) Orthogonal cutting mechanisms of graphite/epoxy composite. International Journal of Machine Tools and Manufacture 35 (12):1623-1638
[32] Zarrouk T, Salhi J. E, Nouari M, Salhi M, Atlati S, Salhi N, Makich H (2021) Analysis of friction and cutting parameters when milling honeycomb composite structures. Advances in Mechanical Engineering 13(7) : 16878140211034841.
[33] Turki Y, Habak M, Velasco R, Vantomme P, Aboura Z (2011) Evaluation expérimentale du comportement d'un composite carbone/époxy en usinage. In Congrès français de mécanique. AFM, Maison de la Mécanique, 39/41 rue Louis Blanc, 92400 Courbevoie, France (FR).